Available online at www.sciencedirect.com
ScienceDirect
Journal of Solid State Chemistry 180 (2007) 2323–2334
JOURNAL OF SOLID STATE CHEMISTRY
www.elsevier.com/locate/jssc

$(Mn_{1-x}Pb_x)Pb_{10+y}Sb_{12-y}S_{26-y}Cl_{4+y}O$, a new oxy-chloro-sulfide with ~2 nm-spaced $(Mn,Pb)Cl_4$ single chains within a waffle-type crystal structure

Charlotte Doussier, Yves Moëlo*, Philippe Léone, Alain Meerschaut

Institut des Matériaux Jean Rouxel, UMR 6502 CNRS-Université de Nantes, 2 rue de la Houssinière, BP 32229, 44322 Nantes cedex 03, France

Received 13 March 2007; received in revised form 30 April 2007; accepted 6 May 2007
Available online 21 May 2007

Abstract

The new oxy-chloro-sulfide $(Mn_{1-x}Pb_x)Pb_{10+y}Sb_{12-y}S_{26-y}Cl_{4+y}O$ ($x \in [0.2–0.3]$; $y \in [0.3–1.6]$) was synthesized by dry way at 500–600 °C. A single crystal ~$Mn_{0.7}Pb_{11.0}Sb_{11.3}S_{25.3}Cl_{4.7}O$ indicates a monoclinic symmetry, space group $C2/m$, with $a = 37.480(8)$, $b = 4.1178(8)$, $c = 18.167(4)$ Å, $\beta = 106.37(3)°$, $V = 2690.2(9)$ Å^3, $Z = 2$. Its crystal structure was determined by X-ray single crystal diffraction, with a final $R = 5.11\%$. Modular analysis of the crystal structure reveals a "waffle" architecture, where complex rods with lozenge section delimitate an internal channel filled by a single chain of $(Mn_{0.7}Pb_{0.3})Cl_6$ octahedra connected by opposite edges. Minimal inter-chain distances are close to 18 Å. The rod wall, two-atom thick, presents, in alternation with S atoms, Pb or (Pb,Sb) cations with prismatic coordination in the internal atom layer, while the external atom layer is constituted exclusively by Sb cations with dissymmetric square pyramidal coordination. A $(Pb,Sb)_2S_2$ fragment connects two successive rods along (2 0 1) to form a waffle-type palissadic layer. The unique O position, half filled, presents the same environment than the isolated O positions in the oxy-sulfide $Pb_{14}Sb_{30}S_{54}O_5$, or oxy-chloro-sulfides $Pb_{18}Sb_{20}S_{46}Cl_2O$ and $(Cu,Ag)_2Pb_{21}Sb_{23}S_{55}ClO$. This compound belongs to a pseudo-homologous series of chalcogenides with waffle structure, ordered according to the size of their lozenge shape channel. Such a complex senary compound of the oxy-chloro-sulfide type illustrates the structural competition between three cations, on one hand, and, on the other hand, three anions. This compound is of special interest regarding the 1D distribution of magnetic Mn^{2+} atoms at the ~2 nm scale.

Keywords: Oxy-chloro-sulfide; Manganese; Lead; Antimony; Synthesis; Crystal structure; Homologous series

1. Introduction

Relatively to pure oxides, halogenides or chalcogenides, compounds associating two anions as specific independent constituents, like oxy-chalcogenides or halogeno-chalcogenides, are scarce. Nevertheless, such mixed anionic compounds are of great interest today, as they may often be described as composite structures, with anionic and cationic segregation in distinct building blocks, each one with its specific physical properties, as pointed by Cario [1]. Thus, one of the best example is that of LaCuOS [2], a transparent *p*-type semiconductor.

Reviews on halogeno-chalcogenides of transition elements were presented by different authors [3–5]. Various studies on quaternary compounds of the halogeno-chalcogenosalt type, associating one metal with one pnictogen, were performed recently : $LnSbS_2Br_2$ (Ln = La, Ce) [6,7], $MPnQ_2X$ family (M: Mn, Cd; Pn: Sb, Bi; Q: S, Se; X: Cl, Br, I) [8–12], $Cu_3Bi_2S_3I_3$ [13–15], $Cu_{6.2}PS_5Cl$ [15], Ag/Bi/(S,Se)/Cl compounds [15–18], $HgAs_4S_4I_2$ [19], Hg_3AsS_4Cl and Hg_3AsSe_4Cl [20], Pb_2AsS_3(I,Cl,Br) [21], Al/(Sb,Bi)/(S,Se,Te)/Cl [21–24].

A fortiori, more complex compounds of the oxy-halogeno-chalcogenide type, like synthetic $Eu_{27}Ti_{20}S_{54}X_2O_{12}$ ($X = I_{0.35}Cl_{0.65}$) [25] are rather uncommon. Recently, two compounds of the oxy-chloro-sulfosalt type were discovered as minerals, pillaite, $Pb_{18}Sb_{20}S_{46}Cl_2O$ [26], and pellouxite, $(Cu,Ag)_2Pb_{21}Sb_{23}S_{55}ClO$ [27]. Together with Pb and Sb as

*Corresponding author.
E-mail address: yves.moelo@cnrs-imn.fr (Y. Moëlo).

0022-4596/$ - see front matter © 2007 Elsevier Inc. All rights reserved.
doi:10.1016/j.jssc.2007.05.012

cations, sulfur constitutes the dominant anion, but the crystal structure studies [28,29] proved that minor chlorine and oxygen act as specific constituents. While pillaite is a quinary compound, pellouxite is a senary (or heptary) one, as there is also a single specific (Cu,Ag) position in the structure.

During the study of complex (Fe,Mn) chalcogenides and derivatives of the sulfosalt type with strong 1D magnetic properties [$MPb_4Sb_6S_{14}$, MSb_2S_4, $MPnQ_2X$ family (*M*: Mn, Fe; *Pn*: Sb, Bi; *Q*: S, Se; *X*: Cl, Br, I)] [10,30], a new oxy-chloro-sulfide with general composition $(Mn_{1-x}Pb_x)Pb_{10+y}Sb_{12-y}S_{26-y}Cl_{4+y}O$ (called hereafter "Mn-OClS") was obtained. In its crystal structure, the 1D organization of magnetic Mn^{2+} is strongly enhanced, with ~2 nm-spaced $(Mn,Pb)Cl_4$ chains. Its crystal chemistry is detailed here.

2. Experimental section

2.1. Synthesis

The studied compound "Mn-OClS" was first obtained (sample A) as a by-product by solid state reaction (ceramic) method from a mixture of FeS, $MnCl_2$, PbS and Sb_2S_3 in the 1/3/2/1 ratios, in order to obtain an ill-defined natural chloro-sulfosalt, $\sim(Mn_{1-x}Fe_x)_2PbSbS_3Cl_3$ [31,32]. Products were put under atmosphere into a silica tube and sealed under vacuum; the synthesis was performed at 500 °C during 10 days.

Single crystal study of rare fibres isolated from the bulk permitted to detect the new compound "Mn-OClS", and to determine its chemical composition, $\sim MnPb_{10}Sb_{12}S_{26}Cl_4O$. The weak oxygen content (0.34 wt.%) revealed by this study was apparently provided from oxidation traces within the reagents. On this basis, two new syntheses (B and C) were performed in a similar way without FeS, and with a starting composition close to the stoichiometric one given above (600 °C; MnS, $PbCl_2$, PbS and Sb_2S_3 — 1/2/10/5 and 1/2/8/6 ratios; 10 and 15 days respectively). A last attempt, performed adding oxygen as MnO (600 °C; MnO, $PbCl_2$, PbS and Sb_2S_3 — 1/2/8/6 ratios; 10 days), failed to obtain "Mn-OClS" (see Section 3.1). All final products were complex, fine grained mixtures of chloro- and oxy-chloro-sulfosalts of Pb and Sb, with or without minor Mn.

2.2. Chemical analysis

Chemical analyses of "Mn-OClS" and associated phases were performed on polished sections, first with a SEM equipped with an energy dispersive spectrometer (EDS). However, because of the overlapping of Pb, S and Cl emission lines using an EDS, and despite the use of a deconvolution program, there is a relatively high error on the measured weight concentration for these elements. Such a difficulty is ruled out through the analysis with electron probe microanalysis (EPMA) equipped with wavelength dispersive spectrometers (WDS). Only the analysis of oxygen is subject to uncertainty, due to its low concentration and to chemical artefacts. For instance, in scainiite, $Pb_{14}Sb_{30}S_{54}O_5$ [33,34] the oxygen content (theoretically 0.96 wt%) was clearly confirmed by EPMA. But when the measured oxygen content decreases down to 0.4 wt% or less, it may also be an artefact, due to the easy formation of an oxidation film at the polished surface of the sulfide. In this case, only the crystal structure study can prove the presence of oxygen, due to its localization on a specific atom position, as it will be shown for "Mn-OClS".

2.3. Crystallographic studies

Due to the chemical and crystallographic complexity of final products, X-ray powder diagrams were useless for the characterization of associated phases. Minute individual fibres were rarely observed, but only the first synthesis A provided fibres suitable for the X-ray single crystal study of "Mn-OClS". It crystallizes with monoclinic symmetry, space group *C*2/*m* (No. 12), with $a = 37.480(8)$, $b = 4.1178(8)$, $c = 18.167(4)$ Å, $\beta = 106.37(3)^\circ$, $V = 2690.2(9)$ Å^3, $Z = 2$. According to the specific position of the oxygen atom with a half site occupancy factor (s.o.f.), there must be a 2*b* superstructure, like in structures of related minerals pillaite, $Pb_{18}Sb_{20}S_{46}Cl_2O$ [28], pellouxite, $(Cu,Ag)_2Pb_{21}Sb_{23}S_{55}ClO$ [29] and scainiite, $Pb_{14}Sb_{30}S_{54}O_5$ [34]. Unfortunately, the quality of the studied crystal was not good enough to solve it. Table 1 gives the crystallographic data obtained on the studied fibre.

Table 1
Crystallographic Data for "Mn-OClS"

Chemical formula	$Mn_{0.72}Pb_{10.97}Sb_{11.31}S_{25.31}Cl_{4.69}O$
Formula weight (g mol^{-1})	4683.22
Crystal size (mm^3)	$0.008 \times 0.100 \times 0.010$
Crystal shape/colour	Needle/black
Temperature (K)	293(2)
Space group	*C*2/*m* (No. 12)
a (Å)	37.480(8)
b (Å)	4.1178(8)
c (Å)	18.167(4)
β (°)	106.37(3)
V (Å^3)	2690.2(9)
Z	2
μ (Mo-*K*α) (mm^{-1})	41.14
D_c (g cm^{-3})	5.782
No. unique reflns	4414
No. observed reflns ($I \geqslant 2\sigma(I)$)	2915
No. refined parameters	196
R_{int}	10.87%
Final R_1/wR ($I \geqslant 2\sigma(I)$)	5.11%/9.82%
GOF	1.018
Residual electronic density (e Å^{-3})	+2.83, −2.12

$R_1 = \Sigma||F_0| - |F_c||/\Sigma|F_0|$.

$wR = \left[\Sigma w(|F_0| - |F_c|)^2/\Sigma w|F_0|^2\right]^{1/2}$.

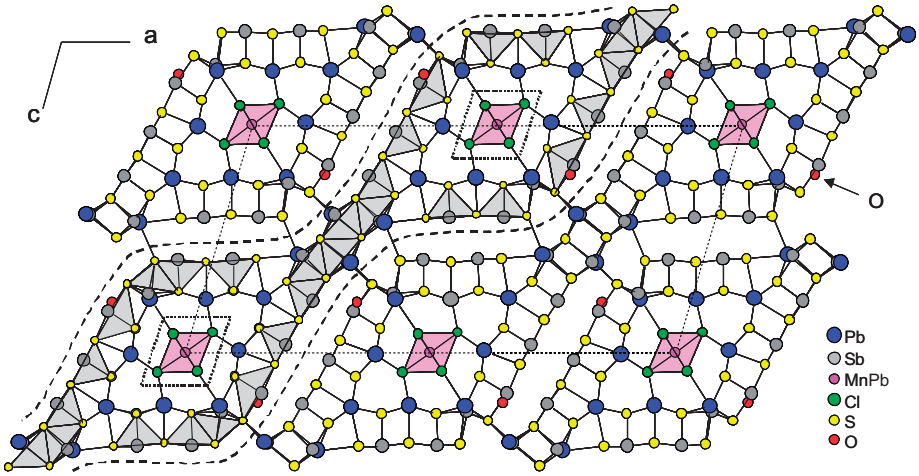

Fig. 1. Projection of the crystal structure of "Mn-OClS" along *b*, with delimitation of the oblique palissadic constitutive layer.

Fig. 1 gives the projection of the structure along *b*. In the course of the structure determination, some uncertainties were removed taking into account EPMA data as well as bond valence calculations according to Brese and O'Keeffe [35]. First, it appears that the anions bound to the unique Mn position correspond to Cl exclusively, and not to S. Correlatively, the Mn position ought to integrate a heavier atom, Sb or Pb. Considering Sb would have given a too low Mn s.o.f. (0.38 Mn against 0.71 in EPMA of sample A), as well as a strong underestimation of the bond valence sum (BVS). On the contrary, a mixed (Mn,Pb) site well agrees with EPMA (Mn/Pb = 0.72/0.28 against 0.71/0.29 in EPMA).

The Cl content given by EPMA of A (4.36 at.) significantly overpasses the 4 Cl atoms around the (Mn,Pb) position. According to crystal structure studies on Pb–Sb chloro-sulfides [36,37] one knows that Cl can substitute for S, however, the precise distribution of this Cl excess among specific S positions could not be solved.

Examination of Fourier-difference residual peaks led us to locate one oxygen position near Sb(5). By comparison with the structures of $Pb_{18}Sb_{20}S_{46}Cl_2O$ (pillaite) or $(Cu,Ag)_2Pb_{21}Sb_{23}S_{55}ClO$ (pellouxite), and in order to preclude too a high *U* value, an half occupancy factor was applied. Correlatively, the mean Sb(5) position has been split along *b* ((*x*,*y*,*z*) and (*x*,−*y*,*z*), with *y* close to 0), with a s.o.f. of 0.50 for each position. Positions of Sb(1), Sb(2), S(6), S(8) and S(9) were also split.

Correlatively, there are three mixed (Pb,Sb) sites (Pb and Sb with distinct sub-positions within the same polyhedra — see Table 2), where the Pb/Sb ratios have been adjusted to respect the charge balance as well as the homogeneity of *U* values. Pb s.o.f. always overpass Sb ones. The final structural formula is $Mn_{0.72}Pb_{10.97}Sb_{11.31}S_{25.31}Cl_{4.69}O$. Finally, one obtains a reliability factor $R = 5.11\%$. Coordinates of atom positions and their equivalent/isotropic displacement parameters ($U_{eq/iso}$) are given in Table 2.

3. Results

3.1. Chemical composition

In run A, the main product was the synthetic equivalent of the mineral observed by Dobbe [31], with a chemical composition close to $Mn_{1.8}Fe_{0.2}PbSbS_3Cl_3$ [32]. All the iron introduced as FeS in the starting mixture was fixed within this phase, without any significant content in co-existing "Mn-OClS". In runs B and C, "Mn-OClS" was one among the main components, together with other Pb–Sb chloro-sulfosalts, but the complexity of the mixtures, as well as of the resulting X-ray powder diagrams, precluded any precise measurement of the yield of the reactions.

Table 3 gives the results of EPMA on selected areas of "Mn-OClS" from syntheses A, B and C. Each sample appears homogeneous; on the basis of a total of 23 cations, samples A, B and C give the formulas $Mn_{0.79}Pb_{11.80}Sb_{10.41}S_{23.77}Cl_{5.79}O$, $Mn_{0.71}Pb_{11.59}Sb_{10.69}S_{24.43}Cl_{5.07}O$ and $Mn_{0.72}Pb_{10.58}Sb_{11.71}S_{25.48}Cl_{4.36}O$, respectively (adding one oxygen atom according to the crystal structure study). One can point out that, without oxygen, the charge balance indicates a significant excess of positive charges (+5.8%, +5.1% and +4.3% for A, B and C, respectively), while adding one oxygen atom, this charge balance (+1.9%, +1.4% and +0.7%, respectively) is in agreement with the precision of EPMA (± 2.0%, for a precision of ± 1.0% on the weight total) [38].

Relatively to sample A, samples B and C are slightly depleted with Mn, but the main difference is a Pb and Cl depletion, and an Sb and S enrichment from A to C. These differences will be discussed later on, on the basis of the crystal structure.

Paradoxically, while "Mn-OClS" was synthesized in runs A, B and C with oxygen as traces, it was not observed in the run starting with oxygen as an oxide (MnO). MnO did react, but the final product was a

Table 2
Atom coordinates (e.s.d.s.) and equivalent isotropic displacement parameters $U_{eq/iso}$ (in Å^2) for "Mn-OClS" at Room Temperature

Atom	site	x	y	z	$U_{eq/iso}$
Pb1	4i	0.4891(1)	0	0.2331(1)	0.031(1)
Pb2	4i	0.3716(1)	0	0.2384(1)	0.033(1)
Pb3	4i	0.3908(1)	0	0.0090(1)	0.031(1)
Pb4/*Sb6*	4i	0.3289(1)/*0.3184(5)*	0	0.4286(1)/*0.426(1)*	0.029(1)
Pb5/*Sb7*	4i	0.7157(3)/*0.723(1)*	0	0.3931(5)/*0.396(2)*	0.050(1)
Pb6/*Sb8*	4i	0.6031(1)/*0.6100(3)*	0	0.2343(2)/*0.259(1)*	0.033(1)
Sb1	8j	0.0696(1)	0.052(1)	0.4072(1)	0.037(1)
Sb2	8j	0.9583(1)	0.054(2)	0.4093(1)	0.039(1)
Sb3	4i	0.7702(1)	0	0.2267(1)	0.036(1)
Sb4	4i	0.7984(1)	0	0.0342 (1)	0.035(1)
Sb5	8j	0.1809(1)	0.044(2)	0.1802(1)	0.036(2)
Mn/*Pb7*	2a	0	0	0	0.032(1)
Cl1	4i	0.5357(1)	0	0.0824(3)	0.044(1)
Cl2	4i	0.9559(1)	0	0.0875(3)	0.036(1)
S1	4i	0.0492(1)	0	0.2664(2)	0.023(1)
S2	4i	0.9378(1)	0	0.2700(3)	0.025(1)
S3	4i	0.8345(1)	0	0.3107(3)	0.025(1)
S4	4i	0.8632(1)	0	0.1065(3)	0.025(1)
S5	4i	0.1163(1)	0	0.1058(2)	0.025(1)
S6	8j	0.8410(1)	0.057(3)	0.7013(3)	0.030(3)
S7	4i	0.6905(1)	0	0.0521(3)	0.037(1)
S8	8j	0.2864(1)	0.055(2)	0.1412(3)	0.023(2)
S9	8j	0.2565(1)	0.042(7)	0.3258(3)	0.025(5)
S10	4i	0.7915(1)	0	0.4959(3)	0.032(1)
S11	4i	0.4107(1)	0	0.4110(3)	0.034(1)
S12	4i	0.5116(1)	0	0.3961(3)	0.034(1)
S13	4i	0.6163(1)	0	0.4014(3)	0.034(1)
O	4i	0.679(1)	0	0.220(2)	0.036(6)

S.o.f. (%): Pb4/*Sb6* = 84/16; Pb5/*Sb7* = 73/27; Pb6/*Sb8* = 77/23; Mn/*Pb7* = 72/28; Sb1, Sb2, Sb5, S6, S8, S9 and O = 50%.

Table 3
Electron microprobe analysis of "Mn-OClS" in Samples A, B and C

	Wt%						Atom ratio (basis : Mn + Pb + Sb = 23 at)						
	Mn	Pb	Sb	S	Cl	Total[a]	Mn	Pb	Sb	S	Cl	Ev	Ev_{cor}
A1	0.97	50.86	26.83	15.98	4.31	99.29	0.84	11.68	10.48	23.70	5.78	6.2	2.3
A2	0.99	50.75	27.19	16.12	4.34	99.73	0.85	11.58	10.56	23.77	5.80	6.0	2.2
A3	0.91	50.93	26.92	16.27	4.32	99.69	0.79	11.69	10.52	24.14	5.79	4.5	0.8
A4	0.85	51.73	25.99	15.70	4.21	98.82	0.74	12.00	10.26	23.53	5.70	6.6	2.7
A5	0.87	51.20	26.23	16.00	4.26	98.88	0.76	11.88	10.36	24.00	5.77	4.8	1.1
A6	0.87	51.79	26.09	15.74	4.36	99.19	0.76	11.97	10.27	23.52	5.89	6.3	2.4
Mean A	*0.91*	*51.21*	*26.54*	*15.97*	*4.30*	*99.27*	*0.79*	*11.80*	*10.41*	*23.78*	*5.79*	*5.8*	*1.9*
σA	*0.06*	*0.45*	*0.50*	*0.22*	*0.06*	*0.39*	*0.05*	*0.17*	*0.13*	*0.25*	*0.06*	*0.9*	
B1	0.82	49.58	28.10	16.67	3.68	99.19	0.71	11.35	10.94	24.66	4.92	5.0	1.3
B2	0.84	50.52	27.30	16.46	3.82	99.28	0.72	11.61	10.67	24.44	5.12	5.0	1.2
B3	0.81	51.33	26.71	16.26	3.83	99.28	0.71	11.82	10.47	24.20	5.16	5.4	1.6
Mean B	*0.82*	*50.48*	*27.37*	*16.46*	*3.77*	*99.25*	*0.71*	*11.59*	*10.69*	*24.43*	*5.07*	*5.1*	*1.4*
σB	*0.01*	*0.87*	*0.70*	*0.21*	*0.09*	*0.05*	*0.01*	*0.24*	*0.24*	*0.23*	*0.13*	*0.3*	
C1	0.87	47.07	30.08	17.29	3.32	98.97	0.74	10.66	11.60	25.31	4.40	4.7	1.0
C2	0.83	46.65	30.78	17.63	3.16	99.39	0.71	10.50	11.79	25.65	4.15	4.2	0.6
C3	0.82	46.40	30.26	17.31	3.39	98.51	0.70	10.57	11.73	25.47	4.52	4.1	0.5
Mean C	*0.84*	*46.71*	*30.37*	*17.41*	*3.29*	*98.96*	*0.72*	*10.58*	*11.71*	*25.48*	*4.36*	*4.3*	*0.7*
σC	*0.02*	*0.34*	*0.36*	*0.19*	*0.12*	*0.44*	*0.02*	*0.08*	*0.10*	*0.17*	*0.19*	*0.3*	

Standards (element—*emission line*): Mn metal (Mn K_α); PbS (Pb M_α), Sb_2S_3 (Sb L_α), FeS_2 (S K_α); $Pb_5(PO_4)_3Cl$ (Cl K_α).

[a]Adding 0.34 wt% oxygen, according to the crystal structure study. Valency balance Ev (%) = $100 \times [(\Sigma val.^+) - (\Sigma val.^-)]/|\Sigma val.^-|$. Ev_{cor}: adding one oxygen atom.

complex mixture of ill-defined chloro-sulfosalts and oxy-chloro-sulfosalts.

3.2. Description of the crystal structure

According to Fig. 1, the basic building block in the crystal structure of "Mn-OClS" is a rod parallel to *b*, with a lozenge section. It has the developed structural formula $(Mn,Pb)Pb_6(Pb,Sb)_6Sb_{10}(S,Cl)_{26}Cl_4(O_{0.5})_2$. The heart of the rod corresponds to a $(Mn,Pb)Cl_4$ single chain, corresponding to the connection of $(Mn,Pb)Cl_6$ octahedra by opposite edges. This chain is surrounded by two mono-atomic covers derived from $(1\,0\,0)_{PbS}$ slabs, the inner one with 6 Pb and 2 (Pb,Sb) as cations, the external one with 10 Sb and 2 (Pb,Sb) sites.

Two adjacent rods are connected by a $(Pb,Sb)_2S_2$ fragment (Fig. 1), to form a palissadic layer parallel to (2 0 1). The undulated surface of such a layer presents essentially Sb as cations, in dissymmetric square pyramids, with their lone electron pair directed outside, towards a symmetric surface of Sb atoms from the adjacent layer, according to the SnS archetype [39]. As a result, such a connection between two layers corresponds to an interface of weak bonding (probably also a cleavage surface), that justifies this modular description of "Mn-OClS" as a waffle structure. Such a general architecture remembers those of zeolites, or of manganese oxides with tunnel structure (hollandite group). Nevertheless, in "Mn-OClS", the $[(Mn,Pb)Cl_4]_\infty$ chain, filling the "channel" of the rod, is connected to the inner wall of the channel wall via relatively strong Cl–Pb bonds.

The unique oxygen position is located on this surface (Fig. 1); it is symmetrically bound up and down along *b* to Sb(5) in split positions, with short and long O–Sb distances of 2.022(1) and 2.359(1) Å, respectively (Fig. 2). The half occupancy of this oxygen position corresponds to the alternation along *b* of one oxygen atom and one vacancy, as exemplified previously in the structures of $Pb_{14}Sb_{30}S_{54}O_5$ [34], $Pb_{18}Sb_{20}S_{46}Cl_2O$ [26] and $(Cu,Ag)_2Pb_{21}Sb_{23}S_{55}ClO$ [27]. Correlatively, to obtain a good BVS for the oxygen atom, when present, it must be bound to the two Sb(5) atoms at short distance ($BVS_O = 1.90$ valence unit – Table 4), while the vacancy position is correlated to the two long distances to Sb(5) at 2.359(1) Å.

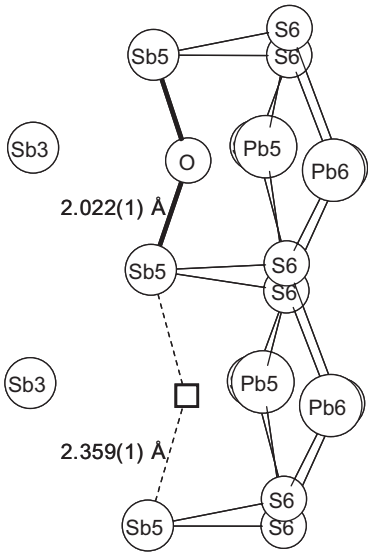

Fig. 2. Environment of the oxygen atom, and its alternation with a vacancy (open square) along *b*.

The mixed unique (Mn,Pb) position, bound only to chlorine atoms, forms an original single chain of $(Mn,Pb)Cl_6$ octahedra, connected via opposite edges (Fig. 3). Such a similar chain with sulfur as anion exists in orthorhombic $MnSb_2S_4$ [40] and its monoclinic dimorph [41], as well as in $MnPb_4Sb_6S_{14}$ [30] and with oxygen as anion in $MnSb_2O_4$ [42]. Here the Mn-Mn inter-chain distances are very high (Fig. 4): 18.17 Å as a minimum along *c*, 18.85 Å along *a*, and 22.12 Å along [102].

In this chain, the presence of minor Pb together with Mn seems a little bit surprising, due to the large difference of their ionic radii, even if one knows that Mn and Pb may present the same octahedral coordination with S, as for

Table 4
Bond valences for selected atoms

Atom *i*	Atom *j*	d_{ij} (Å)	v_{ij}	S.o.f.	Multip.	
Pb1	S1	2.984	0.31	× 1	× 2	0.62
	S2	3.020	0.28	× 1	× 2	0.56
	S12	2.841	0.46	× 1	× 1	0.46
	Cl1	3.306	0.12	× 1	× 2	0.24
					BVS =	*1.88*
Pb2	S2	3.149	0.20	× 1	× 2	0.40
	S3	2.988	0.31	× 1	× 2	0.61
	S4	3.108	0.22	× 1	× 2	0.44
	S8	3.191	0.18	× 1	× 2	0.45
	S11	3.064	0.25	× 1	× 1	0.25
					BVS =	*2.15*
Pb3	S4	3.079	0.24	× 1	× 2	0.48
	S5	2.889	0.40	× 1	× 2	0.80
	S5	2.934	0.35	× 1	× 1	0.35
	Cl1	3.203	0.16	× 1	× 2	0.32
					BVS =	*1.95*
Mn1/Pb7	Cl1	2.598	0.28/0.83	× 0.72/0.28	× 2	0.86
	Cl2	2.672	0.23/0.68	× 0.72/0.28	× 4	1.42
					BVS =	*2.28*
Cl1	Pb1	3.306	0.12	× 1	× 2	0.24
	Pb3	3.203	0.16	× 1	× 2	0.32
	Mn1/Pb7	2.598	0.28/0.83	× 0.72/0.28	× 1	0.43
					BVS =	*0.99*
Cl2	Pb6	3.173	0.18	× 0.77	× 1	0.14
	Mn1/Pb7	2.672	0.23/0.68	× 0.72/0.28	× 2	0.71
					BVS =	*0.85*
O	Sb5	2.022	0.88	× 2	× 1	1.76
	Pb5	3.060	0.08	× 0.73	× 1	0.06
	Pb6	2.929	0.11	× 0.77	× 1	0.08
					BVS =	*1.90*

v_{ij}: bond valence for the (*i*, *j*) atom pair. Only $v_{ij} \geqslant 0.06$ were considered for the bond valence sum (*BVS*).

instance in cubic MnS and PbS (NaCl archetype); but also, such a Mn-for-Pb substitution (solid solution) is known in the mineral shadlunite, (Pb,Cd,Mn)(Fe,Cu)$_8$S$_8$ [43], related to the pentlandite archetype, where isolated regular octahedra contain divalent Pb, Cd or Mn in variable ratios. Furthermore, similar PbI_4 single chains are present in the sulfo-halide $Pb_5S_2I_6$ [44].

Thus, the incorporation of minor Pb on the Mn position is probably necessary due to steric constraints. In a regular Mn–*A* octahedron (*A*: anion), the ideal Mn–*A* distance decreases from 2.606 Å (Mn-S) to 2.536 Å (Mn–Cl), and down to 2.196 Å (Mn–O) (Table 5). But, when comparing the geometry of MnA_6 octahedra in the four compounds with such single chains (Table 5 and Fig. 5), there is a regular increase of the mean Mn–*A* value from $MnSb_2O_4$ to $MnSb_2S_4$ and $MnPb_4Sb_6S_{14}$, and finally "Mn-OClS". The highest value for the (Mn,Pb)Cl$_6$ octahedron (2.647 Å) is clearly due to the presence of Pb (ideal Pb–Cl = 2.936 Å). The dissymmetry of Mn–*A* bonds is given by the ratio between the two apical bonds (M_{ap}, perpendicular to the chain elongation) and the four equatorial ones (M_{eq}); it is pronounced only for $MnPb_4Sb_6S_{14}$ (M_{ap}/M_{eq} = 1.103). On the other hand, there is a positive correlation between the regular increase of the metal intra-chain distance from 2.999 Å ($MnSb_2O_4$) up to 4.118 Å ("Mn-OClS"), and the decrease of the *A*–Mn–*A* elongation angle (Fig. 5), that indicates a stretching of the octahedron parallel to the chain elongation. Such a stretching conflicts with the small size of pure $MnCl_6$ octahedron, and necessitates the incorporation of minor Pb for the stabilization of such a chain within the waffle-type matrix.

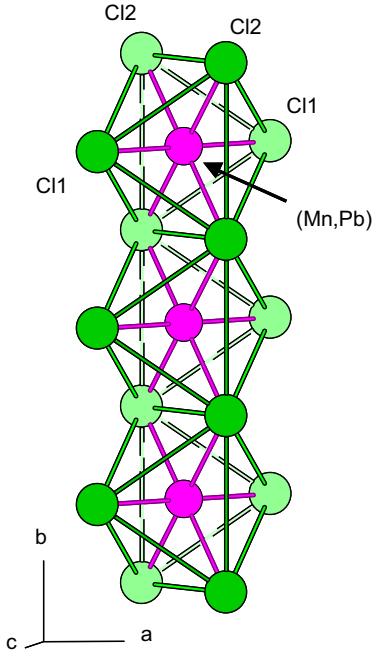

Fig. 3. The (Mn,Pb)Cl$_4$ single chain in "Mn-OClS".

Inside the rod, the chain, delimited by Cl^- anions, is necessarily negatively charged, corresponding to $[(Mn,Pb)Cl_4]^{2-}$; these negative charges are neutralized by bonds with Pb^{2+} cations, on the inner side of the rod wall.

3.3. Crystal chemistry of "Mn-OClS" solid solution

Without Cl on S positions, the ideal formula of "Mn-OClS" would be $(Mn_{1-x}Pb_x)Pb_{10}Sb_{12}S_{26}Cl_4O$. According to EPMA, a Cl excess over 4 atoms is correlated to a Pb excess, as well as an Sb and S deficit, according to the classic heterovalent substitution scheme: $Sb^{3+} + S^{2-} \rightarrow Pb^{2+} + Cl^-$ [36,37,45]. The general formula becomes:

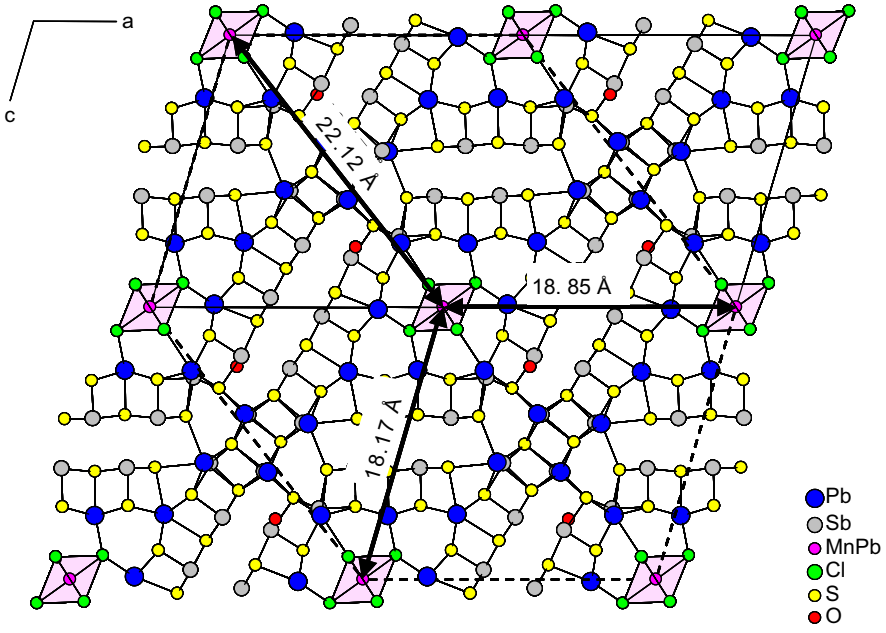

Fig. 4. (Mn,Pb)Cl$_4$ inter-chain distances in "Mn-OClS".

Table 5
Geometry of Mn octahedra in compounds with MnA_4 single chains

	$MnSb_2O_4$	$MnSb_2S_4$	$MnPb_4Sb_6S_{14}$	"Mn-OClS"
Ideal octahedral Mn-A (Å)	2.196	2.606	2.606	2.536 (Mn)
(A: O, S, Cl)				2.936 (Pb)
Mean 6 bonds (Å)	2.145	2.604	2.613	2.647
Mean 2 apical M_{ap} (Å)	2.205	2.549	2.445	2.598
Mean 4 equat. M_{eq} (Å)	2.115	2.632	2.697	2.672
M_{ap}/M_{eq}	0.959	1.033	1.103	1.028
Elongation angle (°)	89.69(1)	86.76(1)	83.60(1)	79.18(1)
Mn-Mn intra-chain (Å)	2.999(1)	3.823(1)	4.022(1)	4.118(1)

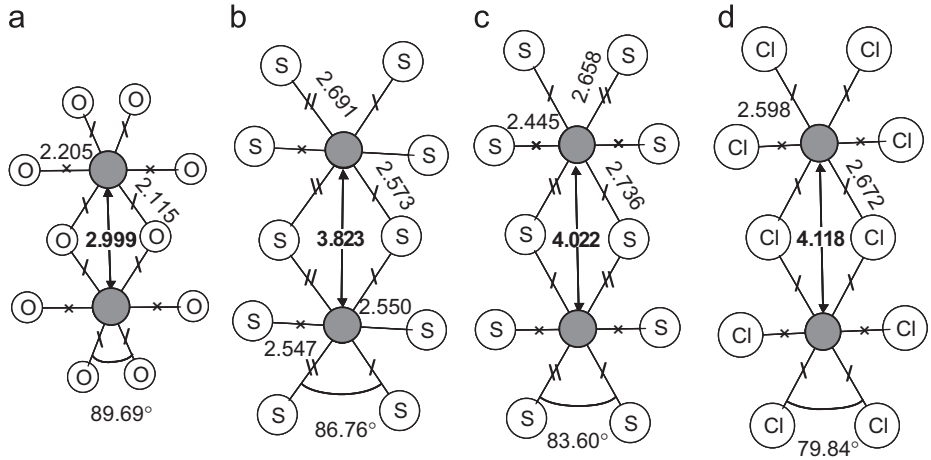

Fig. 5. Geometry of MnA_6 octahedra in single chains within the structures of $MnSb_2O_4$ (a), $MnSb_2S_4$ (b), $MnPb_4Sb_6S_{14}$ (c) and "Mn-OClS" (d). Mn–A and Mn–Mn distances (Å) are indicated, as well as the A–Mn–A elongation angles.

$(Mn_{1-x}Pb_x)Pb_{10+y}Sb_{12-y}S_{26-y}Cl_{4+y}O$. On the basis of EPMA (Table 3), one has $x \cong 0.2/0.3/0.3$ and $y \cong 1.6$ /1.3/ 0.3 for samples A, B and C, respectively.

4. Comparative modular analysis: related structures with waffle architecture

Some natural and synthetic sulfides and chloro-sulfides present also crystal structures with the same type of waffle architecture. They can be presented and compared to "Mn-OClS" on the basis of the rod geometry, notably the size of their channel.

4.1. Vurroite, $Pb_{20}Sn_2(Bi,As)_{22}S_{54}Cl_6$

Vurroite is a complex chloro-sulfide, recently discovered in high temperature fumaroles at Vulcano (Italy) [46]. The general architecture of its structure (Fig. 6a) [47,48] is very close to that of "Mn-OClS" (Fig. 6c), despite the differences in their chemistry:

- the internal single chain has the formula (Sn,Bi)S_4;
- at the convex margin of the layer, the Sb–$O_{0.5}$–S–S–Sb sequence is replaced by the sequence (Bi,As)–S–Cl–S–(Bi,As), with correlatively a symmetry plane giving an orthorhombic symmetry; here, the doubling of the atom thickness of the wall is possible owing to the presence of As^{3+} with marked lone electron pair activity, like for Sb^{3+} in "Mn-OClS";
- there is only one, and not two, M–S atom pair in vurroite for the connection between two successive rods, in relationship with the symmetry plane.

4.2. Pillaite, $Pb_{18}Sb_{20}S_{46}Cl_2O$

Fig. 6b represents the constitutive complex layer of pillaite, $Pb_{18}Sb_{20}S_{46}Cl_2O$, also of the palissadic type [28]. The general architecture is very similar, even in the details, for instance concerning the unique marginal oxygen position with identical coordination. But, while in "Mn-OClS" the heart of a rod is a single chain of octahedra with composition (Mn,Pb)Cl_4, in pillaite, this heart has the composition $Pb_2Sb_4S_{10}Cl_2$, and is three (pseudo-)octahedra large and two (pseudo-)octahedra wide. A second difference is the connection between two successive rods, which needs an additional $(Pb,Sb)_2S_2$ fragment for "Mn-OClS" relatively to pillaite.

Thus, there is a homologous relationship between the basic rods of "Mn-OClS" and pillaite. That of pillaite is an expanded derivative of that of "Mn-OClS" by a 2D-inflation

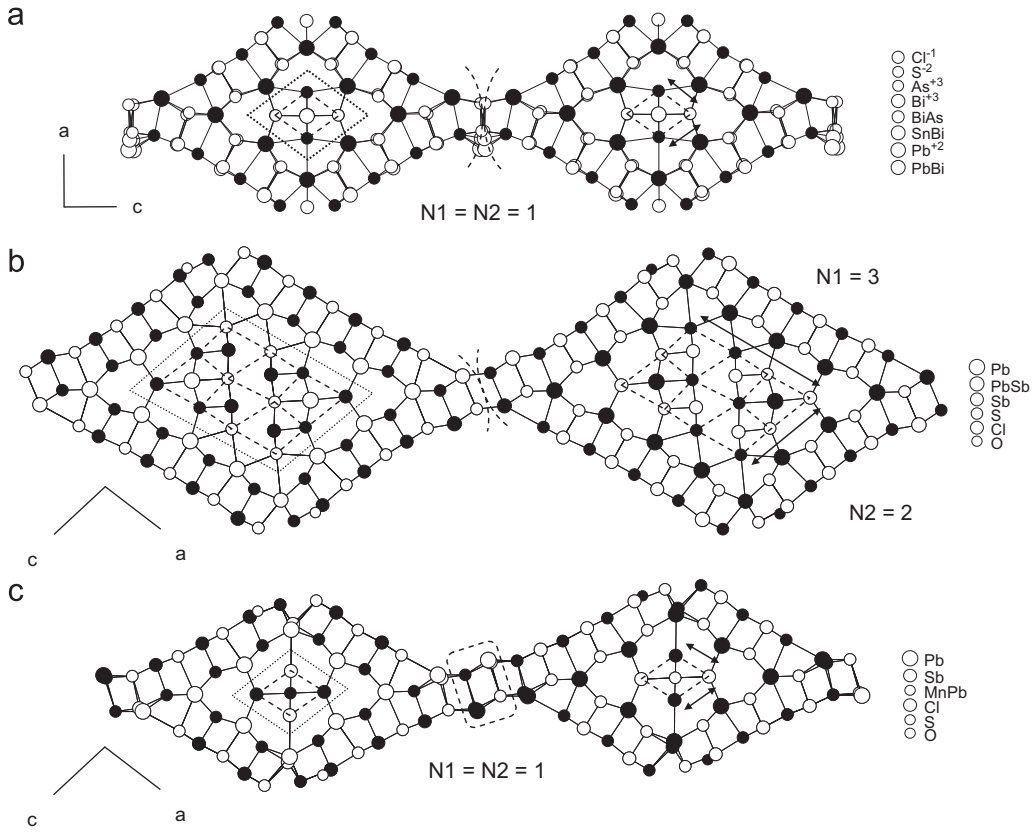

Fig. 6. Comparison between the palissadic constitutive layers of vurroite (a) pillaite (b) and "Mn-OClS" (c) Open and filled circles correspond to a shift equal or close to half the (sub-) periodicity along the projection direction.

operation. Considering the rod of pillaite, the two sides of the lozenge heart can be defined by the numbers N_1 and N_2 (Fig. 6b), with $N_1 = 2$ and $N_2 = 3$ in this case. The general formula of such a rod can be thus obtained:

- heart: $(N_1–N_2)\ M + [(N_1 + 1)(N_2 + 1)]\ A$ (M: divalent and trivalent cations); (1)
- internal mono-atomic cover: $2\ [(N_1 + 1) + (N_2 + 1)]\ M + 2\ [(N_1 + 1) + (N_2 + 1) + 1]\ A$; (2)
- external mono-atomic cover : $2\ [(N_1 + 2) + (N_2 + 2)]\ M + 2\ [(N_1 + 2) + (N_2 + 2) + 1]\ A + 2\ O_{0.5}$.

Without cation differentiation, the general formula for a (N_1,N_2) rod thus becomes:

- $\Sigma\ M = (N_1–N_2) + 4\ (N_1 + N_2) + 12$;
- $\Sigma\ A = (N_1 + 1)(N_2 + 1) + 4\ (N_1 + N_2) + 16$;
- plus 1O.

With $(N_1,N_2) = (2,3)$, one obtains the reduced formula $M_{38}A_{48}O$ of pillaite. The homologous rod of "Mn-OClS" corresponds to $(N_1,N_2) = (1,1)$, that gives the simplified formula $M_{21}A_{28}O$. Complementarily, two cations and two anions, corresponding to the stretching of the rod connection, must be added to obtain the final reduced formula of "Mn-OClS", that is $M_{23}A_{30}O$.

Such a determination of a sub-homologous relationship between two crystal structures, that permits to define a general derivation rule, is consequently a way for the prediction of new structural types. Such an approach has been developed previously in the field of complex lead sulfosalts (mineral and related synthetics) [49,50] and recently applied in the field of solid chemistry for similar synthetic compounds [51,52].

4.3. Waffle structures with thinned rod wall

In "Mn-OClS", $Pb_{20}Sn_2(Bi,As)_{22}S_{54}Cl_6$ (vurroite) and $Pb_{18}Sb_{20}S_{46}Cl_2O$ (pillaite), the double wall separating two adjacent rod hearts is four-atom thick. This is due to the presence, in the two internal atom slabs, of Sb^{3+} or As^{3+}, with a strong stereochemical activity of their lone-electron pair. Such a role played by Sb^{3+} for the splitting in two of M_2S_2 layers is well known in the group of 2D-misfit chalcogenides, as exemplified by the pairs cylindrite $[(Pb,Sb)_2S_2]_{0.69}(Sn,Fe)S_2$/franckeite $[(Pb,Sb)_4S_4]_{0.68}(Sn,Fe)S_2$ [53], and synthetics $[(Pb,Nb)_2S_2]_{0.57}NbS_2/[(Pb,Sb)_4S_4]_{0.57}NbS_2$ [54].

Inversely, there are compounds of the waffle type, without Sb^{3+} or As^{3+}, where the double wall is reduced to two-atom thick (that is a one-atom-thick rod wall). Their general formula would correspond to the sum of

formulas (1) and (2) above, that is: $[(N_1 \cdot N_2) + 2(N_1 + N_2) + 4]\ M + [(N_1 \cdot N_2) + 3(N_1 + N_2) + 7]A$.

$Pb_2La_xBi_{8-x}S_{14}$ ($x \sim 2.1$) [55] appears as the primitive derivative of pillaite, $Pb_{18}Sb_{20}S_{46}Cl_2O$ (Fig. 7a), with the same rod heart ($N_1,N_2 = 2,3$ — M_6S_{12}), surrounded with a one-atom-thick wall ($M_{14}S_{16}$). As pointed by these authors, the compound $La_4Bi_2S_9$ is also of the primitive type (Fig. 7b) [56], with a rod heart of ($N_1,N_2 = 1,2 - M_2S_6$), and a one-atom-thick wall ($M_{10}S_{12}$).

The primitive derivative of "Mn-OClS" (heart: $M(S/X)_4$; wall: M_8S_{10}) is not known. Nevertheless, the chalcogenides of the $RE_6In_{1-x}Ti_{1-x}S_{12}$ series (RE = Nd, Sm, Gd) [57] present a waffle structure which can be considered as a compressed variant of this primitive derivative (Fig. 7c):

- the heart of the lozenge channel is filled by a $(In,Ti)S_4$ infinite chain;
- the wall of the rod is one-atom thick;
- the short connection between two successive channels along a is realized by a common (Ti,In) atom forming a second infinite chain $(Ti,In)S_4$.

In the (N_1,N_2) = (0,0) and (0,1) simplest rods, the channel contains only anions (one and two atom files, respectively). The crystal structures of Pb_4SeBr_6 (orthorhombic *Imm*2) [44] and U_3Te_5 (orthorhombic *Pnma*) [58] represent distorted derivatives of these ideal primitive homologues (Fig. 8).

Table 6 presents all these compounds with waffle structure according to the rod size. One can see that the unit cell volume increases rapidly due to the 2D inflation ((N_1,N_2) pair), as well as to the specific role of Sb^{3+} and As^{3+}.

5. Discussion

The new compound "Mn-OClS" is a very didactic example of a senary compound where there is a strong crystal chemical segregation due to specific chemical affinities/competitions between three cations, on the one hand, and, on the other hand, three anions. The oxygen atom is strongly bound to Sb, which one is preferentially bound to S; Pb is bound to S and Cl, while Mn is bound only to Cl. A similar case was described for $(Cu,Ag)_2Pb_{21}Sb_{23}S_{55}ClO$ (pellouxite), where there is a coupling between the unique (Cu,Ag) site and the unique mixed (Cl,S) site, while the unique O atom is also bound to Sb with the same configuration [27].

According to its crystal structure, "Mn-OClS" thus corresponds to a mixture of the binary compounds Sb_2S_3, Sb_2O_3, PbS, $PbCl_2$ and $MnCl_2$, but with probably a very narrow stability field within the phase equilibrium diagram of such a pseudo-quinary system. As a consequence, a small excess of one among these five components may be sufficient to overpass the limits of the stability field of "Mn-OClS", that would explain the failure of the experimental run with MnO as a starting product.

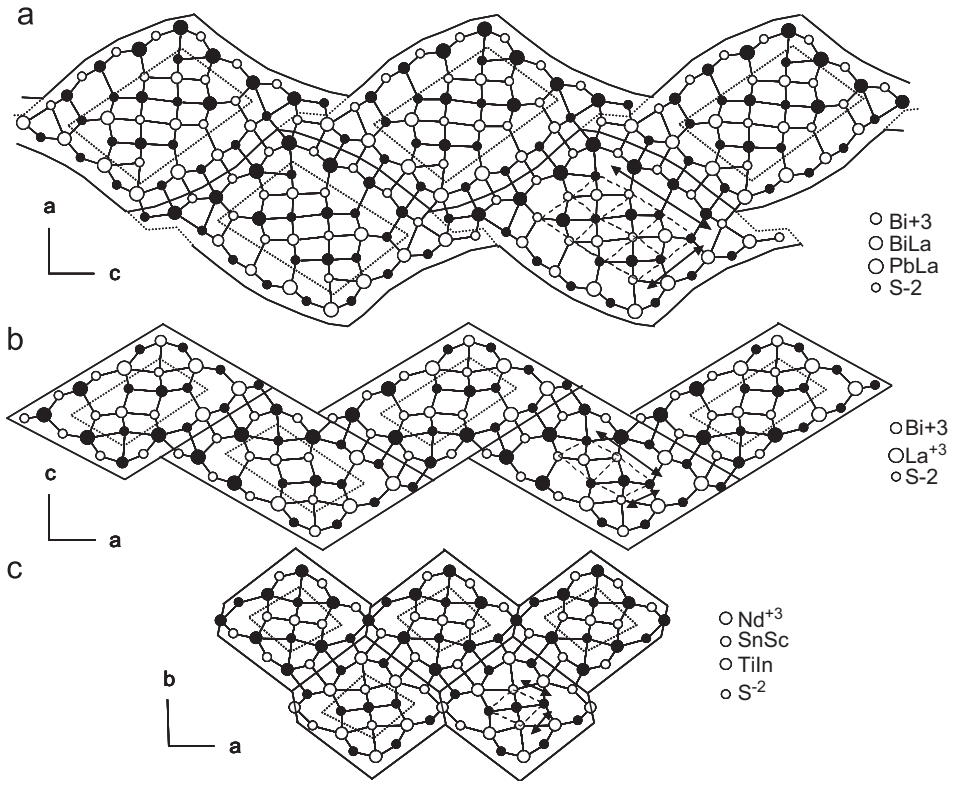

Fig. 7. Waffle architectures with one-atom-thick rod wall of $Pb_2La_xBi_{8-x}S_{14}$, the primitive structure of pillaite, with a $(N_1,N_2) = (3,2)$ heart (a); $La_4Bi_2S_9$, with a $(N_1,N_2) = (2,1)$ heart (b); and Nd_6InTiS_{12}, a compressed primitive structure related to "Mn-OClS", with a $(N_1,N_2) = (1,1)$ heart (c).

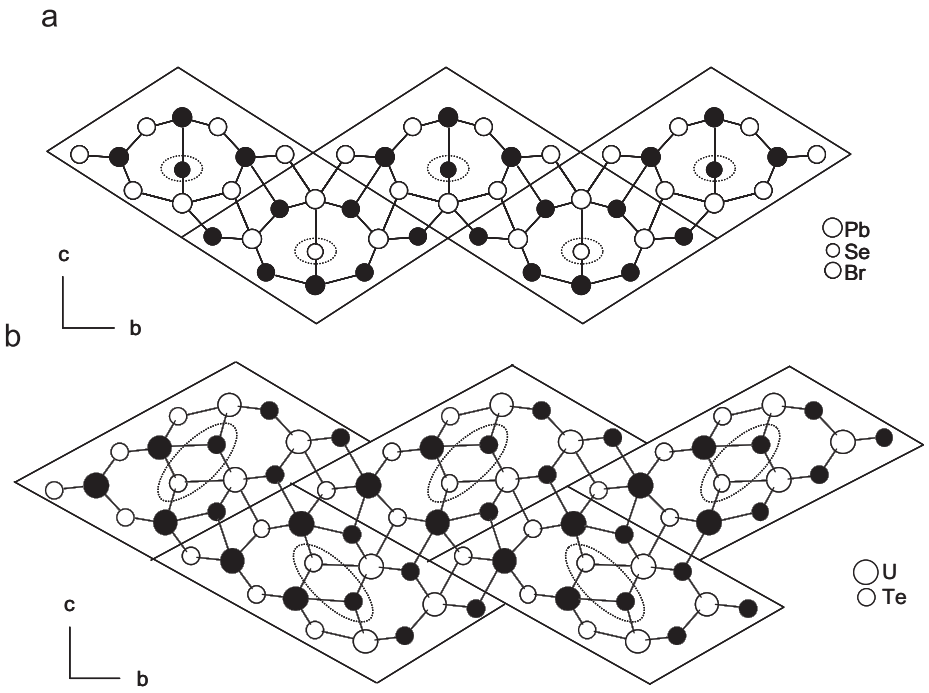

Fig. 8. Waffle architectures of Pb_4SeBr_6 with a $(N_1,N_2) = (0,0)$ heart (a) and U_3Te_5 with a $(N_1,N_2) = (0,1)$ heart (b).

Table 6
Classification of chalcogenides with waffle structure

N_1 N_2	Compound	Column formula	*Pn*	V[a] (Å^3)
0.0	Synth. [44]	Pb_4SeBr_6	–	334
0.1	Synth. [58]	U_6Te_{10}	–	476
1.1	Synth. [57]	Nd_6InTiS_{12}	–	437
1.1	"Mn-OClS"	$Mn_{0.72}Pb_{10.97}Sb_{11.31}S_{25.31}Cl_{4.69}O$	Sb	1345[b]
1.1	Vurroite [48]	$Pb_{10}Sn(Bi.As)_{11}S_{27}Cl_3$	As	1294[b]
1.2	Synth. [56]	$La_8Bi_4S_{18}$	Bi	743
2.3	Synth. [55]	$Pb_4La_{2x}Bi_{16-2x}S_{28}$	Bi	1210
2.3	Pillaite [28]	$Pb_{18}Sb_{20}S_{46}Cl_2O$	Sb	2197[b]

Pn: Pnictogen.
[a]Reduced volume for one column, with the elongation (sub)periodicity close to 4 Å.
[b]Rod wall splitting due to Sb or As lone electron pair.

The 1D distribution of Mn atoms (at the +II oxidation state) is of high interest for magnetic study. In complex sulfosalts, similar ("iso-topologic") single chains of MnS_6 octahedra connected by opposite edges, with variable inter-chain distances (d_{out}), are known in $MnSb_2S_4$ (d_{out} = 6.650(2) Å) and in $MnPb_4Sb_6S_{14}$ (d_{out} = 12.364(1) Å). This induces specific 3D magnetic transitions [30,59], and the possibility of a Haldane system with spin $S = 2$ was envisaged for the Fe isotype of $MnPb_4Sb_6S_{14}$ [60], but excluded according to the magnetic structure evidenced by neutron diffraction [61]. In "Mn-OClS", there is the same 1D distribution of (Mn,Pb)Cl_6 octahedra, but here the minimum inter-chain distance increases up to about 18 Å, that constitutes to our knowledge the highest 1D gap among inorganic compounds. Nevertheless, the partial substitution of Pb to Mn disrupts the Mn ordering along the chain; it thus appears necessary to search for chemical derivatives of "Mn-OClS" in order to match the elongation of the Mn octahedron of this chain to the periodicity of the waffle matrix, and thus to obtain Mn-pure chains.

In such a Mn-pure derivative, the drastic increase of the inter-chain distance would strongly bring down the temperature of 3D magnetic ordering, and open the temperature gap between 1D and 3D magnetic ordering, if present. Considering the Mn–Mn intra- and inter-chain distances (d_{in} and d_{out}), in $MnSb_2O_4$, (d_{in} = 2.99 Å, d_{out} = 6.21 Å), 3D magnetic ordering appears at 60 K [62]. In monoclinic $MnSb_2S_4$ (d_{in} = 3.82 Å, d_{out} = 6.65 Å), 3D magnetic ordering appears downwards, at 25 K [32]. In benavidesite, $MnPb_4Sb_6S_{14}$ (d_{in} = 4.02 Å, d_{out} = 12.44 Å), 1D ordering appears first at 30 K, and 3D ordering secondly at 6 K [30,61]. In the hypothetic derivative of "Mn-OClS" with Mn-pure chains (d_{in} ~4.1 Å, d_{out} ~18.2 Å), the 1D ordering temperature would

not decrease significantly, but the 3D magnetic ordering would probably be possible only down to 1 K or less.

For $S = 2$ Haldane conjecture, it would be of special interest to obtain the Fe-pure isotype of "Mn-OClS", but the stabilization of this Fe derivative may be precluded by steric constraints. As pointed above in "Mn-OClS", Mn is partially substituted (at less about 20%) by the bigger Pb cation, due to such constraints. According to ionic radii, the $FeCl_6$ octahedron is a little bit smaller (mean distances of 2.466 and 2.536 Å for $Fe^{2+}Cl_4$ and $Mn^{2+}Cl_4$ with regular octahedral coordination, respectively), that would be a higher obstacle for the synthesis of the intra-chain Fe-pure pole.

More generally, "Mn-OClS" and related compounds with waffle structures illustrate the interest of the crystal chemical approach of comparative modular analysis for combinatory synthesis in solid chemistry. Here the search for new structure types must take into account different building operators. Some of them are classic, like the relative sizes of cations (or cation–anion bonds), or the principle of charge neutrality (local and global). Others are more particular, like the relative competition between different cations against different anions, or the specific role of Sb^{3+} or As^{3+} for the splitting in two of the waffle matrix. At a higher level, modular analysis permits the definition of homologous series, and the derivation of new building blocks through 2D-inflation operations. Consideration of all these constraints is necessary to optimize the prediction and synthesis of multi-cationic and anionic compounds.

6. Conclusion

Despite the presence of minor Pb in the Mn-rich single chain, the new compound "Mn-OClS" is to be compared with nano-structured materials, as its architecture presents parallel mono–atomic files of magnetic Mn^{2+} regularly distributed at a large, ~2 nm scale within a non-magnetic matrix. Among low-dimensional inorganic systems, "Mn-OClS" is an original prototype for the experimental and theoretical study of magnetic chains. Nevertheless, the control of the synthesis of such a compound, as well as of chemical derivatives (purity, as well as non-mixing of intra-chain sites filled by Mn or other possible transition metal), is a pre-requisite for such physical studies.

Appendix A. Supplementary Materials

Supplementary data associated with this article can be found in the online version at doi:10.1016/j.jssc.2007.05.012.

Appendix B

Further details of the crystal structure investigation may be obtained from Fachinformationszentrum Karlsruhe, 76344 Eggenstein-Leopoldshafen, Germany (fax: (+49) 7247-808-666; e-mail: crysdata(at)fiz-karlsruhe.de, http://www.fiz-karlsruhe.de/request_for_deposited_data.html) on quoting the CSD number 418201.

References

[1] L. Cario, H. Kabbour, A. Meerschaut, Chem. Mater. 17 (2005) 234–236.
[2] K. Ueda, S. Inoue, S. Hirose, H. Kawazoe, H. Hosono, Appl. Phys. Lett. 77 (2000) 2701–2703.
[3] D.A. Rice, Coord. Chem. Rev. 25 (1978) 199–227.
[4] M.J. Atherton, J.H. Holloway, Adv Inorg. Chem. Radiochem. 22 (1979) 171–198.
[5] J. Fenner, A. Rabenau, G. Trageser, Adv Inorg. Chem. Radiochem. 23 (1980) 330–425.
[6] D. Gout, S. Jobic, M. Evain, R. Brec, J. Solid State Chem. 158 (2001) 218–226.
[7] P.F. Poudeu-Poudeu, T. Söhhnel, M. Ruck, Z. Anorg. Allg. Chem. 630 (2004) 1276–1285.
[8] O. Tougait, J.A. Ibers, A. Mar, Acta Crystallogr. C 59 (2003) 77–78.
[9] C. Doussier, P. Léone, Y. Moëlo, Solid State Sci 6 (2004) 1387–1391.
[10] C. Doussier, Y. Moëlo, P. Léone, Solid State Sci 8 (2006) 652–659.
[11] A. Pfitzner, M. Zabel, F. Rau, Z. Anorg. Allg. Chem. 631 (2005) 1439–1441.
[12] L. Wang, Y.C. Hung, S.J. Hwu, H.J. Koo, M.H. Whangboo, Chem. Mater. 18 (2006) 1219–1225.
[13] T. Balic-Zunic, K. Mariolacos, K. Friese, E. Makovicky, Acta Crystallgor. B 61 (2005) 239–245.
[14] T. Nilges, A. Pfitzner, Z. Kristallogr. 220 (2005) 281–294.
[15] M. Ruck, Z. Anorg. Allg. Chem. 628 (2002) 453–457.
[16] M. Ruck, Z. Anorg. Allg. Chem. 628 (2002) 1537–1540.
[17] M. Ruck, P.F. Poudeu Poudeu, T. Soehnel, Z. Anorg. Allg. Chem. 630 (2004) 63–67.
[18] P.F. Poudeu Poudeu, M. Ruck, J. Solid State Chem. 179 (2006) 3636–3644.
[19] M.F. Bräu, A. Pfitzner, Angew. Chem. 45 (2006) 4464–4467.
[20] J. Beck, S. Hedderich, K. Köllisch, Inorg. Chem. 39 (2000) 5847–5850.
[21] M. Zelenski, T. Balic-Žunić, L. Bindi, A. Garavelli, E. Makovicky, D. Pinto, F. Vurro, Amer. Mineral. 91 (2006) 21–28.
[22] J. Beck, S. Schlüter, M. Dolg, Angew. Chem. 40 (2001) 2287–2290.
[23] J. Beck, S. Schlüter, N. Zotov, Z. Anorg. Allg. Chem. 630 (2004) 2512–2519.
[24] J. Beck, S. Schlüter, Z. Anorg. Allg. Chem. 631 (2005) 569–574.
[25] L. Cario, J.A. Cody, C. Deudon, A. Meerschaut, C. R. Acad. Sci. Paris IIc (1998) 115–121.
[26] P. Orlandi, Y. Moëlo, A. Meerschaut, P. Palvadeau, P. Eur. J. Mineral. 13 (2001) 605–610.
[27] P. Orlandi, Y. Moëlo, A. Meerschaut, P. Palvadeau, P. Léone, Eur. J. Mineral. 16 (2004) 839–844.
[28] A. Meerschaut, P. Palvadeau, Y. Moëlo, P. Orlandi, P., Eur. J. Mineral. 13 (2001) 779–790.
[29] P. Palvadeau, A. Meerschaut, P. Orlandi, Y. Moëlo, Eur. J. Miner. 16 (2004) 845–855.
[30] P. Léone, L.M. Le Leuch, P. Palvadeau, P. Molinié, Y. Moëlo, Solid State Sci 5 (2003) 771–776.
[31] R. Dobbe, Ph.D. Thesis, Vrije University, The Netherlands, 1994.
[32] C. Doussier-Brochard, Ph.D. Thesis, Nantes University, France, 2006.
[33] P. Orlandi, Y. Moëlo, A. Meerschaut, P. Palvadeau, Eur. J. Mineral. 11 (1999) 949–954.
[34] Y. Moëlo, A. Meerschaut, P. Orlandi, P. Palvadeau, Eur. J. Mineral. 12 (2000) 835–846.
[35] N.E. Brese, M. O'Keeffe, Acta Crystallogr. B 47 (1991) 192–197.
[36] V.V. Kostov, J. Macíček, Eur. J. Mineral. 7 (1995) 1007–1018.
[37] V.V. Kostov-Kytin, R. Petrova, J. Macíček, Eur. J. Mineral. 9 (1997) 1191–1197.

[38] Y. Moëlo, N. Mozgova, P. Picot, N. Bortnikov, Z. Vrublevskaya, Tschermaks Mineral. Petrogr. Mitt. 32 (1984) 271–284.
[39] E. Makovicky, Eur. J. Mineral. 5 (1993) 545–591.
[40] K. Bente, A. Edenharter, Z. Kristallog. 186 (1989) 31–33.
[41] A. Pfitzner, D. Kurowski, Z. Kristallogr. 215 (2000) 373–376.
[42] J.R. Gavarri, G. Calvarin, B. Chardon, J. Solid State Chem. 47 (1983) 132–142.
[43] T.L. Evstigneeva, A.D. Genkin, N.V. Troneva, A.A. Filimonova, A.I. Tsepin, Zap. Vses. Mineral. Obshchestva 102 (1973) 63–74.
[44] B. Krebs, Z. Anorg. Allg. Chem. 396 (1973) 137–151.
[45] Y. Moëlo, O. Balitskaya, N. Mozgova, A. Sivtsov, Eur. J. Mineral. 1 (1989) 381–390.
[46] A. Garavelli, N.N. Mozgova, P. Orlandi, E. Bonaccorsi, D. Pinto, Y. Moëlo, Y.S. Borodaev, Can. Mineral. 43 (2005) 703–711.
[47] D. Pinto, Ph.D. Thesis, Bari University, Italy, 2004.
[48] D. Pinto, Plinius 31 (2005) 197–202.
[49] E. Makovicky, W.G. Mumme, J.A. Watts, Can. Mineral. 15 (1977) 339–348.
[50] E. Makovicky, Z. Kristallogr. 173 (1985) 1–23.
[51] M.G. Kanatzidis, Acc. Chem. Res. 38 (2005) 359–368.
[52] A. Mrotzek, M.G. Kanatzidis, J. Solid State Chem. 167 (2002) 299–301.
[53] E. Makovicky, B.G. Hyde, Mater. Sci. Forum 101 (1992) 1–100.
[54] A. Lafond, A. Meerschaut, Y. Moëlo, J. Rouxel, C. R. Acad. Sci. 322 (1996) 165–173.
[55] L. Iordanidis, M.G. Kanatzidis, Inorg. Chem. 40 (2001) 1878–1887.
[56] C. Ecrepont, M. Guittard, J. Flahaut, J. Mater. Res. Bull. 23 (1988) 37–42.
[57] Y.C. Hung, S.J. Hwu, Chem. Mat. 7 (1995) 1661–1667.
[58] O. Tougait, M. Potel, H. Noël, J. Solid State Chem. 139 (1998) 356–361.
[59] D. Kurowski, Ph.D. Thesis, Regensburg, Germany, 2003.
[60] Y. Matsushita, Y. Ueda, Inorg. Chem. 42 (2003) 7830–7838.
[61] P. Léone, G. André, C. Doussier, Y. Moëlo, J. Magn. Magn. Mater. 284 (2004) 92–96.
[62] R. Chater, J.R. Gavarri, J. Solid State Chem. 59 (1985) 123–131.